Letter

Integrability is generic in homogeneous U(1)-invariant nearest-neighbor qubit circuits

Marko Žnidarič, Urban Duh, and Lenart Zadnik
Physics Department, Faculty of Mathematics and Physics, University of Ljubljana, 1000 Ljubljana, Slovenia

(Received 14 October 2024; revised 19 June 2025; accepted 23 June 2025; published 7 July 2025)

Integrability is an exceptional property believed to hold only for systems with fine-tuned parameters. Contrary, we explicitly show that in homogeneous nearest-neighbor qubit circuits with a U(1) symmetry, i.e., circuits that repeatedly apply the same magnetization-conserving two-qubit gate, this is not the case. There, integrability is generic: All such brickwall qubit circuits are integrable, even with a randomly selected gate. We identify two phases with different conservation laws, transport properties, and strong zero edge modes. Experimentally important is the fact that varying any one of the parameters in the generic U(1) gate, one will typically cross the critical manifold that separates the two phases. Finally, we report on an unconventional time-reversal symmetry causing the system with open boundary conditions to be in the orthogonal class, while the one with periodic boundary conditions is in the unitary class.

DOI: 10.1103/tqy8-ynpd

Introduction. Integrable models are indispensable in theoretical physics because they offer a rare glimpse into the full analytical structure of otherwise complex phenomena. Integrability is an exact mathematical concept related to the existence of a sufficient number of conserved quantities. In classical physics a system with d degrees of freedom is said to be integrable if it has (at least) d conserved quantities in involution, a canonical example being the Kepler's two-body problem. Quantum integrability is often described similarly—one has to have a sufficient number of local conserved operators [1]. Finding integrable quantum many-body systems is particularly important due to the exponential complexity of numerical approaches. Two notable examples of many-body integrable systems are the Heisenberg spin-1/2 model of quantum magnetism and the two-dimensional (2D) Ising model of phase transitions. All these models are solvable by the so-called Yang-Baxter formalism [2], a definition of integrability which we use herein. A particularly appealing feature of the Yang-Baxter integrability is that the full integrable structure follows from a solution of a Yang-Baxter equation, i.e., from the so-called R matrix [see Eq. (3)]. That structure includes an infinite number of local conserved operators which can be used to analytically study the dynamics, the transport phenomena, etc.—see Ref. [3] for a collection of reviews.

With a rapid progress of quantum computers and simulators [4–7], where the natural setting is that of a circuit made of local gates, having integrable quantum circuits is desirable. Same-gate circuits, in which one repeatedly applies the same unitary gate, are especially appealing, since they are simpler to realize experimentally, and they can be theoretically studied using the Floquet formalism. Inspired by integrable light-cone discretizations of quantum field theories [8,9], some integrable Floquet systems have been found in the recent decade, for example, a nearest-neighbor circuit with a gate of an XXX or XXZ type [10–12]. Those initial findings have since been extended in several directions [13–15], including higher-dimensional local space [16], unitary gates with a larger range [17–21], as well as nonunitary circuits [22,23]. Nevertheless, integrability is still regarded as a fine-tuned property. For instance, a generic perturbation of any of the above known integrable Floquet systems is believed to break integrability, leading to chaos [24,25]. In this Letter we show that this is not always the case. Specifically, using the R matrix of the asymmetric six-vertex model [26–28], we will explicitly show that U(1)-invariant circuit composed of a magnetization-conserving (MC) two-qubit Haar-random gate arranged in a brickwall pattern is integrable (see Fig. 1). Note that the U(1) symmetry alone does not in any way guarantee integrability. On the contrary, a typical system with magnetization conservation is chaotic, e.g., the 1D XXZ spin chain in a staggered field, or the 2D Hubbard model.

Magnetization-conserving circuits. The circuits we study consist of two-qubit unitary gates that preserve magnetization, i.e., they have a U(1) symmetry. The gate can be expressed as $U = \mathrm{e}^{-\mathrm{i}\tau h}$, where

$$h_{1,2} = \sigma_1^{\mathrm{x}}\sigma_2^{\mathrm{x}} + \sigma_1^{\mathrm{y}}\sigma_2^{\mathrm{y}} + \Delta\sigma_1^{\mathrm{z}}\sigma_2^{\mathrm{z}} + M\left(\sigma_1^{\mathrm{z}} + \sigma_2^{\mathrm{z}}\right) + B\left(\sigma_2^{\mathrm{z}} - \sigma_1^{\mathrm{z}}\right) + D\left(\sigma_1^{\mathrm{x}}\sigma_2^{\mathrm{y}} - \sigma_1^{\mathrm{y}}\sigma_2^{\mathrm{x}}\right) + A\,\mathbb{1} \quad (1)$$

acts on two neighboring qubits, labeled by 1 and 2. Parameters A and M, associated with two trivially conserved operators, i.e., the identity $\mathbb{1}$ and the magnetization $\sigma_1^{\mathrm{z}} + \sigma_2^{\mathrm{z}}$, are irrelevant, as they only determine the phase. One therefore has four relevant parameters: the gate duration τ, the anisotropy Δ, the staggered magnetic field B, and the Dzyaloshinskii-Moriya coupling D (current). While we will return to the above parametrization later, for the proof of the circuits' integrability

Published by the American Physical Society under the terms of the Creative Commons Attribution 4.0 International license. Further distribution of this work must maintain attribution to the author(s) and the published article's title, journal citation, and DOI.

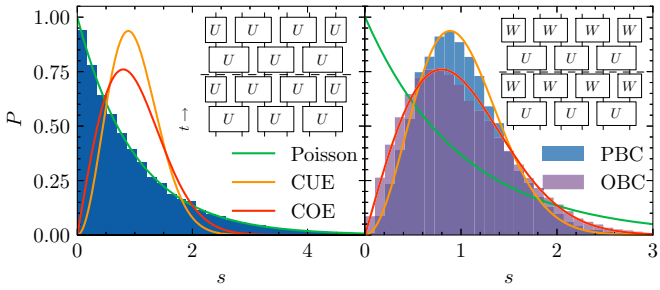


FIG. 1. Level-spacing distribution of eigenphases of a Floquet propagator can often suggest integrability or chaos [29,30]. A homogeneous magnetization-conserving qubit circuit with a Haar-random gate and periodic boundary conditions (PBC, left) shows Poissonian statistics, suggesting integrability, while a circuit with two different gates in consecutive layers (right) is chaotic with an additional time-reversal symmetry (see Appendix A in the Supplemental Material [31]) in the case with open boundary conditions (OBC). Numerics is done on $L = 16$ qubits, resolved over magnetization (OBC and PBC), momentum (PBC), and space-time symmetry [32] (homogeneous).

it will be easier to express the gate using the standard Hurwitz parametrization [35] of a Haar-random MC unitary [36]:

$$U_{\text{Haar}} = \begin{bmatrix} e^{i\delta} & 0 & 0 & 0 \\ 0 & & & 0 \\ 0 & & V & 0 \\ 0 & 0 & 0 & e^{i\delta} \end{bmatrix}, \quad V = e^{i\alpha} \begin{bmatrix} \sin\varphi e^{-i\chi} & \cos\varphi e^{-i\vartheta} \\ \cos\varphi e^{i\vartheta} & -\sin\varphi e^{i\chi} \end{bmatrix}. \tag{2}$$

Here, we removed the irrelevant phase corresponding to the conserved magnetization (the field M), which allows us to write the same phase in the two corners of U_{Haar}. A generic U_{Haar} is obtained by picking the parameters from a distribution that is uniform with respect to an invariant U(1)-preserving measure $d\mu \sim d(\sin^2\varphi)d\chi\, d\alpha\, d\vartheta\, d\delta$, with $\alpha, \chi, \vartheta, \delta \in [0, 2\pi)$, and $\varphi \in [0, \pi/2)$. Quantum circuits utilizing such MC random gates have received a lot of attention recently—see, e.g., Refs. [37–39]. To establish integrability of a circuit we need to find a unitary solution of the Yang-Baxter equation that will be equal to our gate U_{Haar}, and show that it can span *all* MC Haar-random gates. The latter is not obvious [40], despite the integrability [26–28] of all translationally invariant Hamiltonians with local densities (1) [41]. Once that is done, all nice integrability consequences follow from the Yang-Baxter formalism [2]. In the following, we recall the basic formulation of integrable circuits [11,12].

Integrable circuits. The Yang-Baxter equation in its braid form is

$$\check{R}_{1,2}(x)\check{R}_{2,3}(x+y)\check{R}_{1,2}(y) = \check{R}_{2,3}(y)\check{R}_{1,2}(x+y)\check{R}_{2,3}(x), \tag{3}$$

where $\check{R}(-x)\check{R}(x) = \mathbb{1}$ and $\check{R}(0) = \mathbb{1}$. It is the basic building block of integrable systems and a defining equation of $\check{R}$, having many solutions corresponding to different integrable systems. Once a solution $\check{R}$ is found the conserved charges can be constructed with the help of a transfer matrix. While $\check{R}$ can depend on many free parameters one is distinguished as a spectral parameter and is written as the argument x of $\check{R}(x)$. Denoting $R(x) = P\check{R}(x)$, where P is a permutation of two qubits, one constructs a staggered transfer matrix [11,12] acting on L qubits as

$$T(x;u) \equiv \text{tr}_{\mathfrak{a}}[R_{1,\mathfrak{a}}(x_+)R_{2,\mathfrak{a}}(x_-)R_{3,\mathfrak{a}}(x_+)\cdots R_{L,\mathfrak{a}}(x_-)]. \tag{4}$$

Here, the first index $1, \ldots, L$ is a physical index that, as we will shortly see, corresponds to our qubits, while the second index $\mathfrak{a}$ denotes a single auxiliary qubit space over which we trace. $u \in \mathbb{R}$ is a real inhomogeneity parameter, and $x_\pm \equiv x \pm \frac{u}{2}$. Due to the Yang-Baxter equation (3), such transfer matrices commute for different values of the spectral parameter $x \in \mathbb{C}$. The brickwork circuit on L qubits is then obtained as

$$\mathbb{U} = T\left(-\frac{u}{2};u\right)^{-1} T\left(\frac{u}{2};u\right) = \prod_{j=1}^{L/2} U_{2j,2j+1} \prod_{j=1}^{L/2} U_{2j-1,2j}, \tag{5}$$

where the indices are taken modulo L in a circuit with periodic boundary conditions, and it turns out that the U on the right-hand side is exactly equal to $\check{R}$, i.e., $U = \check{R}(u)$, and one can interpret $\mathbb{U}$ as a one-step propagator of a circuit [11]. Because $T(x;u)$ for different parameters x commute (and thus also with $\mathbb{U}$), the conserved charges for a circuit can be obtained via the standard formalism of integrability. Namely, the logarithmic derivatives of the L-qubit transfer matrix $T(x;\frac{u}{2})$ at $x = \pm\frac{u}{2}$ yield two families of local conserved charges, which we denote by $Q^{\pm}_{\ell}(u) \equiv \partial_x^{\ell} \log T(x;u)|_{\pm\frac{u}{2}}$. These charges depend on the inhomogeneity parameter $u \in \mathbb{R}$ and are invariant under translations for an even number of sites. For example, the first logarithmic derivatives give rise to two local charges

$$Q^{+}_{1}(u) = \sum_{j=1}^{L/2} \partial_x[\check{R}_{2j,2j+1}(x_+)\check{R}_{2j+1,2j+2}(x_-)]_{\frac{u}{2}} U^{-1}_{2j,2j+1},$$
$$Q^{-}_{1}(u) = \sum_{j=1}^{L/2} U_{2j,2j+1}\partial_x[\check{R}_{2j-1,2j}(x_+)\check{R}_{2j,2j+1}(x_-)]_{-\frac{u}{2}}, \tag{6}$$

whose local densities act on three adjacent qubits (see Appendix B in the Supplemental Material [31] for their explicit form). A similar property holds also for higher charges: The ℓth conserved charge has local density supported on $r = 2\ell + 1$ neighboring sites. Together with the U(1) charge, i.e., magnetization, we find r charges with support on at most r lattice sites for any odd r.

From U_{Haar} to $\check{R}$ matrix. We will show that U_{Haar} can be parametrized by the known unitary solution of the Yang-Baxter equation (3)—the R matrix of the so-called asymmetric six-vertex model [26–28],

$$\check{R}(u) = e^{i\beta u} \begin{pmatrix} 1 & 0 & 0 & 0 \\ 0 & ib\,e^{-i\xi u} & -a\,e^{-i\theta} & 0 \\ 0 & -a\,e^{i\theta} & ib\,e^{i\xi u} & 0 \\ 0 & 0 & 0 & 1 \end{pmatrix}, \tag{7}$$

where a and b will be expressed in two different forms. In what we call phase I, we will use

$$a_{\text{I}} = \frac{\sin u}{\sin(u + i\rho)}, \quad b_{\text{I}} = \frac{\sinh\rho}{\sin(u + i\rho)}, \tag{8}$$

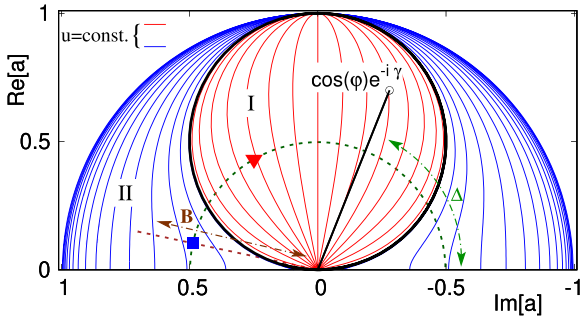


FIG. 2. Two-dimensional projection of the phase diagram. Complex values of $a(u, \rho)$ must span the whole half disk describing possible values of $\cos\varphi e^{-i\gamma}$. Phase I (in red) is separated from phase II (in blue) by the critical manifold (black circle). Curves are lines of constant u, and the blue square and the red triangle are parameters shown in Fig. 3. Green and brown dashed curves show how the circuit moves if one would vary the anisotropy Δ (green), or the staggered field B (brown), fixing all other parameters.

while in phase II we have

$$a_{\mathrm{II}} = \frac{\sinh u}{\sinh(u + i\rho)}, \quad b_{\mathrm{II}} = \frac{\sin\rho}{\sinh(u + i\rho)}. \tag{9}$$

The reason to use two different forms is to always have a parametrization in terms of real parameters only. Alternatively, we could use just one form, say Eq. (8), but with both purely real as well as purely imaginary parameters. Our choice of $\check{R}$, Eqs. (8) and (9), is therefore always parametrized by five real parameters β, ξ, θ, ρ, and u, ensuring unitarity. Notably, it has one parameter more than the integrable Hamiltonian with local density given in Eq. (1), since in the latter the staggered field B cancels out due to translational invariance.

Using $U_{\mathrm{Haar}} = \check{R}(u)$, we will explicitly express the above parameters in terms of Haar angles, thus showing that the $\check{R}$ matrix spans all U_{Haar}. First, we note that, in both phases, a and b satisfy $|a|^2 + |b|^2 = 1$ and, since $u, \rho \in \mathbb{R}$, also $ab^* \in \mathbb{R}$. Therefore one can write $a = \cos\tilde{\varphi}(u, \rho)e^{-i\gamma(u,\rho)}$ and $b = \sin\tilde{\varphi}(u, \rho)e^{-i\gamma(u,\rho)}$. Comparing $\check{R}$ and U_{Haar}, we first deduce the relations

$$\beta u = \delta, \quad \theta = \vartheta, \quad \tilde{\varphi} = \varphi, \tag{10}$$

$$\gamma = \delta - \alpha + \pi. \tag{11}$$

Then, we must find real u and ρ, such that

$$a = \cos\varphi\, e^{-i\gamma}, \quad b = \sin\varphi\, e^{-i\gamma} \tag{12}$$

are satisfied. There is a subtle point here: In order to be able to solve Eq. (12) for all possible angles δ, α, φ with only either a_{I} or a_{II}, we must use a freedom in the Haar block V, Eq. (2). Specifically, since $V(\vartheta + \pi, \chi + \pi, \alpha + \pi, \varphi) = V(\vartheta, \chi, \alpha, \varphi)$ holds, we can always bring γ, Eq. (11), to the interval $\gamma \in [-\frac{\pi}{2}, \frac{\pi}{2})$ (since γ does not depend on ϑ or χ, simply change them and α by an appropriate integer multiple of π). With this reduction, $\cos\varphi\, e^{-i\gamma}$ in Eq. (12) fills the right half of the unit disk, which is exactly the set covered by a_{I} and a_{II} for real u and ρ (see Fig. 2). This freedom in Haar block seems crucial in making the R matrix span all U_{Haar}. Without it, we would have to introduce an additional sign in the R matrix [28]. Using a_{I} and b_{I}, Eq. (8), in Eq. (12), we now obtain

$$u_{\mathrm{I}} = \arccos\left(\frac{\sin\gamma}{\sin\varphi}\right), \quad \rho_{\mathrm{I}} = \operatorname{arccosh}\left(\frac{\cos\gamma}{\cos\varphi}\right), \tag{13}$$

and finally, also $\xi u = \chi - \frac{\pi}{2}$. If, on the other hand, we take a_{II} and b_{II} from Eq. (9), we instead obtain

$$u_{\mathrm{II}} = \operatorname{arccosh}\left(\frac{|\sin\gamma|}{\sin\varphi}\right), \quad \rho_{\mathrm{II}} = s\arccos\left(\frac{\cos\gamma}{\cos\varphi}\right), \tag{14}$$

where $s = \mathrm{sgn}(\sin\gamma)$ is the sign of $\sin\gamma$, and $\xi u = \chi - s\frac{\pi}{2}$. Separation between the two solutions is as follows: If $\cos\varphi < \cos\gamma$ we are in phase I, Eq. (13), while for $\cos\varphi > \cos\gamma$ we are in phase II, Eq. (14).

The two phases. Let us now discuss the physical properties of the two phases. In terms of parameters of the Hamiltonian (1), the condition for phase I reads

$$\left|\frac{\sin(2\tau\Delta)}{\sin(2\tau\sqrt{1 + D^2 + B^2})}\sqrt{1 + \frac{B^2}{1 + D^2}}\right| > 1. \tag{15}$$

A two-parameter integrable XXZ circuit ($D = B = 0$) of Ref. [12] is recovered by setting $\beta = 0$, $\xi = 0$, and $\theta = \pi$. Specifically, the ballistic ("gapless") phase of that circuit is contained in our phase II, and the diffusive ("gapped") one in phase I. The integrable isotropic Heisenberg circuit, discussed in Ref. [11], is contained in the critical manifold, and additionally requires substituting $u \to u\rho$ and taking the limit $\rho \to 0$.

Importantly, compared to the XXZ gates we have an integrable family with four parameters τ, Δ, B, D, and a three-dimensional critical manifold specified by the condition in Eq. (15). On the space of MC gates the critical manifold therefore has a codimension one, which makes these circuits experimentally interesting: Changing an arbitrary parameter, one will typically cross the critical manifold. One particular example is the transition when τ is varied (for the XXZ gate, see Ref. [42]): As seen in Eq. (15), upon changing τ (or, similarly, Δ) one in fact repeatedly oscillates between the two phases, thus encountering an infinite number of such transitions. Such is the case also with D—it essentially just renormalizes the hopping to $\sqrt{1 + D^2}$ (see Appendix A in the Supplemental Material [31]). On the other hand, changing B is qualitatively different. Given parameters, there exists a point of no return B_{crit}: Further increasing B beyond B_{crit}, one can no longer leave phase I, approaching the origin $|a| = 0$ (Fig. 2) as $B \to \infty$ (the origin also corresponds to a continuum limit $\tau \to 0$ of the XXX gate [11]). Finally, we note that, if the unitary gate U_{Haar} is drawn according to the Haar measure, exactly half of the gates will correspond to phase I. If, on the other hand, one draws Hamiltonian parameters [cf. Eq. (1)], the ensemble will be, for nonzero B, biased towards phase I, due to the square root in Eq. (15).

Since phases I and II differ in the analytical structure of the $\check{R}$ matrix, we expect also their physical properties to be different, similarly as for the XXZ gate [12]. To illustrate different physics we touch upon the appearance of localized boundary modes that are robust to all magnetization-preserving gate perturbations, and which are present even at an infinite temperature. Their existence has been established in the gapped

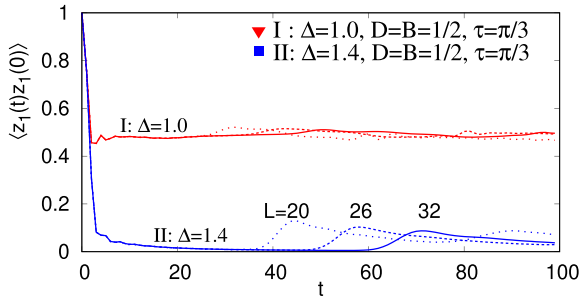


FIG. 3. Infinite-temperature autocorrelation function of a boundary magnetization in the two phases. Strong zero modes exist in phase I (red), while correlations decay for the point in phase II (blue). Gate parameters correspond to the points shown in Fig. 2.

phase of the XXZ spin chain [43], and has been derived also in phase I of the XXZ circuit [44]. In Fig. 3 we numerically demonstrate that the infinite-temperature autocorrelation function of the boundary spin, $\mathrm{tr}[\sigma_1^z(t)\sigma_1^z]/2^L$, does not decay to zero in phase I even in the presence of D and B. Similarly, a fully polarized domain wall state, which is known to be "frozen" in time in the gapped XXZ chain [45], exhibits similar behavior for generic MC gates in phase I. Lastly, in the Ruelle-Pollicott spectra of both phases, discussed below and shown in Fig. 4, one can recognize the quasilocal conserved operators which, for instance, cause fractal ballistic transport in phase II of the XXZ gate. At present, the group structure required to analytically derive them for general parameters of the circuit is not known. The above observations support our conjecture that physical properties can differ between phases I and II.

Ruelle-Pollicott spectrum. We now discuss the method of Ruelle-Pollicott (RP) resonances [46,47], which is incidentally how we realized that MC circuits are integrable. Introducing weak nonunitary perturbation to the propagator and analyzing its spectrum in the limit of zero perturbation, one may find frozen isolated eigenvalues inside the unit circle. Typically expected for chaotic systems, such Ruelle-Pollicott resonances signal exponential decay of correlation functions [24,25]. Here, we apply the method to integrable systems, by writing the operator-evolution propagator in an infinite system, truncating it to r-local translationally invariant operators [48,49], and considering its RP spectrum (for an alternative nonunitarity by weak dissipation, less

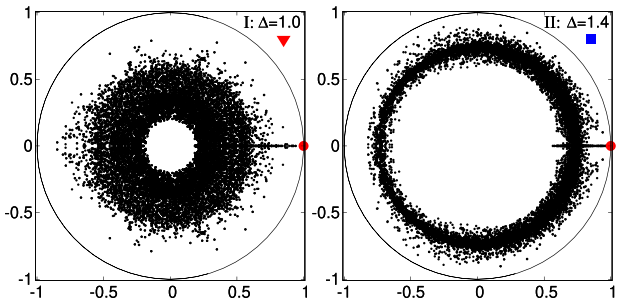


FIG. 4. RP spectrum for the same Hamiltonian parameters as shown in Fig. 3. The red point marks $\lambda = 1$ (seven times degenerate for the shown $r = 7$).

suitable for systems with conservation laws, see, e.g., recent Refs. [50–52]). More precisely, since brickwork circuits are two-site shift invariant, we can consider the sector with a given momentum k, spanned by operators $o_k[q] \equiv \sum_j \mathrm{e}^{\mathrm{i}kj}\mathcal{S}^{2j}q$. Here, $\mathcal{S}$ is a one-site shift and q is a local operator acting on at most r consecutive sites. The matrix elements of the truncated propagator $\mathbb{T}(k)$ between two basis elements $o_k[q]$ and $o_k[q']$ are then

$$[\mathbb{T}(k)]_{q',q} = \sum_{j\in\{-1,0,1\}} \mathrm{e}^{-\mathrm{i}kj}\langle \mathcal{S}^{2j}q'|\mathcal{U}q\rangle, \quad \mathcal{U}q \equiv \mathbb{U}^\dagger q \mathbb{U}, \tag{16}$$

where $\langle q'|q\rangle \equiv \mathrm{tr}(q'^\dagger q)/2^r$, while q and q' run over all r-local operators starting either on the even or odd sites (see Refs. [49,53] for details). A representative spectrum of $\mathbb{T}(k)$ is shown in Fig. 4 for $k = 0$. We find that the eigenvalue 1 is r-times degenerate (for odd r), the corresponding eigenvectors being the magnetization and the local conserved charges $Q_\ell^\pm(u)$ with $2\ell + 1 \leqslant r$ [cf. Eq. (6)]. Another prominent feature are the eigenvalues which, when r is increased, get more numerous and exponentially closer in modulus to 1. The corresponding eigenvectors are quasilocal conserved operators: For a finite r they are almost conserved, the violation coming from their exponential tails. For further details, see Appendix C in the Supplemental Material [31].

Conclusion. We have shown that a two-parameter family of U(1) invariant integrable circuits, for example with the XXZ gate, can be extended to a four-parameter (excluding the field M) integrable family containing all brickwork circuits with magnetization-preserving two-qubit gates. We find this surprising, since integrability is associated with fine tuning, while chaotic dynamics is considered generic. We conjecture that the integrable family described herein is the largest possible among the homogeneous qubit circuits, and is furthermore larger than the largest integrable spin chain class. It could play a similar role in quantum computation as other integrable many-body systems do in their respective domains.

Many new questions are opened, first and foremost being, what are the properties of these models? For instance, for the two-parameter subset describing the integrable XXZ circuit [12] we know that, crossing from one phase to another, spin transport properties in the zero-magnetization sector change drastically. In our extended family we have two new parameters, so one can perhaps expect even richer behavior, e.g., the staggered field B seems to have a qualitatively different effect than the other three parameters. The chiral Dzyaloshinskii-Moriya term could perhaps lead to similar effects of broken space-reflection symmetry as in recently studied circuits and Hamiltonian systems in Refs. [16,54,55].

The critical manifold is also of particular interest. It contains the known [11] one-parameter XXX gate for which Kardar-Parisi-Zhang [56] equilibrium fluctuations of the two-point correlations have been observed [57] due to integrability and SU(2) symmetry [58]. We expect that similar physics can be observed also at nonisotropic values of the parameters ($\Delta \neq 1$).

Yet another open direction are integrable nonunitary circuits [14,22,23] from the same R matrix, but with complex parameters. Here, one should consider Sklyanin's boundary

reflection equations [59], which put constraints on integrable systems with open boundary conditions. Concerning open boundary conditions, the existence of strong zero modes also calls for further studies.

Experimental possibilities are equally exciting. While in the past the XXZ- or XXX-type gates have been targeted [60–62] due to their interesting physics, our results show that any magnetization-conserving gate will do. No fine tuning is therefore required, and what is more, to be at a critical point one just has to vary any generic parameter, such as the gate duration or the anisotropy.

Having a large integrable family of circuits also poses a question regarding robustness of their properties to integrability breaking. Could a slow thermalization in an apparently chaotic model with different MC gates, recently observed in Ref. [63], be related to being close (on average) to the integrable class of circuits discussed here?

We also show the usefulness of the truncated operator propagator—an object usually used in studies of Ruelle-Pollicott resonances of chaotic systems. Compared to the level-spacing statistics, which can be plagued by hard-to-identify symmetries and other issues [30], it directly targets arguably the most important object in integrable systems—the conserved operators—and could be used to identify other new integrable systems.

Lastly, we point at an interesting observation discussed in Appendix A in the Supplemental Material [31], which is relevant for the level-spacing statistics in Fig. 1. Namely, when boundary conditions in a generic nonintegrable (even disordered) brickwall circuit with MC gates are changed from open to periodic, an unconventional time-reversal symmetry is broken, changing the spectral statistics from the orthogonal to the unitary symmetry class.

Acknowledgments. We thank Chiara Paletta, Enej Ilievski, and Tomaž Prosen for useful comments on the manuscript. We acknowledge support by Grants No. J1-4385 and No. P1-0402 from Slovenian Research Agency. L.Z. also acknowledges support by ERC Advanced Grant No. 101096208–QUEST.

[1] J.-S. Caux and J. Mossel, Remarks on the notion of quantum integrability, J. Stat. Mech. (2011) P02023.

[2] R. J. Baxter, *Exactly Solved Models in Statistical Mechanics* (Academic Press, London, 1982).

[3] P. Calabrese, F. H. L. Essler, and G. Mussardo, Introduction to "Quantum integrability in out of equilibrium systems", J. Stat. Mech. (2016) 064001, Special Issue on Quantum Integrability in Out of Equilibrium Systems.

[4] P. N. Jepsen, J. Amato-Grill, I. Dimitrova, W. W. Ho, E. Demler, and W. Ketterle, Spin transport in a tunable Heisenberg model realized with ultracold atoms, Nature (London) **588**, 403 (2020).

[5] D. Wei, A. Rubio-Abadal, B. Ye, F. Machado, J. Kemp, K. Srakaew, S. Hollerith, J. Rui, S. Gopalakrishnan, N. Y. Yao, I. Bloch, and J. Zeiher, Quantum gas microscopy of Kardar-Parisi-Zhang superdiffusion, Science **376**, 716 (2022).

[6] A. Morvan *et al.*, Formation of robust bound states of interacting microwave photons, Nature (London) **612**, 240 (2022).

[7] M. K. Joshi, F. Kranzl, A. Schuckert, I. Lovas, C. Maier, R. Blatt, M. Knap, and C. F. Roos, Observing emergent hydrodynamics in a long-range quantum magnet, Science **376**, 720 (2022).

[8] C. Destri and H. J. De Vega, Light-cone lattice approach to fermionic theories in 2D: The massive Thirring model, Nucl. Phys. B **290**, 363 (1987).

[9] L. D. Faddeev and A. Yu. Volkov, Hirota equation as an example of integrable symplectic map, Lett. Math. Phys. **32**, 125 (1994).

[10] V. Gritsev and A. Polkovnikov, Integrable Floquet dynamics, SciPost Phys. **2**, 021 (2017).

[11] M. Vanicat, L. Zadnik, and T. Prosen, Integrable Trotterization: Local conservation laws and boundary driving, Phys. Rev. Lett. **121**, 030606 (2018).

[12] M. Ljubotina, L. Zadnik, and T. Prosen, Ballistic spin transport in a periodically driven integrable quantum system, Phys. Rev. Lett. **122**, 150605 (2019).

[13] P. W. Claeys, J. Herzog-Arbeitman, and A. Lamacraft, Correlations and commuting transfer matrices in integrable unitary circuits, SciPost Phys. **12**, 007 (2022).

[14] Y. Miao, V. Gritsev, and D. V. Kurlov, The Floquet Baxterization, SciPost Phys. **16**, 078 (2024).

[15] A. Hutsalyuk, Y. Jiang, B. Pozsgay, H. Xu, and Y. Zhang, Exact spin correlators of integrable quantum circuits from algebraic geometry, arXiv:2405.16070.

[16] L. Zadnik, M. Ljubotina, Ž. Krajnik, E. Ilievski, and T. Prosen, Quantum many-body spin ratchets, PRX Quantum **5**, 030356 (2024).

[17] S. Gopalakrishnan, Operator growth and eigenstate entanglement in an interacting integrable Floquet system, Phys. Rev. B **98**, 060302(R) (2018).

[18] Y. Miao and E. Vernier, Integrable quantum circuits from star-triangle relation, Quantum **7**, 1160 (2023).

[19] B. Pozsgay, A Yang–Baxter integrable cellular automaton with a four site update rule, J. Phys. A: Math. Theor. **54**, 384001 (2021).

[20] T. Gombor and B. Pozsgay, Integrable spin chains and cellular automata with medium-range interaction, Phys. Rev. E **104**, 054123 (2021).

[21] V. K. Singh, A. Sinha, P. Padmanabhan, and V. Korepin, Unitary tetrahedron quantum gates, arXiv:2407.10731.

[22] L. Sá, P. Ribeiro, and T. Prosen, Integrable nonunitary open quantum circuits, Phys. Rev. B **103**, 115132 (2021).

[23] C. Paletta and T. Prosen, Integrability of open boundary driven quantum circuits, SciPost Phys. **18**, 027 (2025).

[24] P. Gaspard, *Chaos, Scattering and Statistical Mechanics* (Cambridge University Press, Cambridge, UK, 1998).

[25] D. Braun, *Dissipative Quantum Chaos and Decoherence* (Springer, Berlin, 2001).

[26] K. Sogo, M. Uchinami, Y. Akutsu, and M. Wadati, Classification of exactly solvable two-component models, Prog. Theor. Phys. **68**, 508 (1982).

[27] N. Beisert, L. Fievet, M. de Leeuw, and F. Loebbert, Integrable deformations of the XXZ spin chain, J. Stat. Mech. (2013) P09028.

[28] R. S. Vieira, Solving and classifying the solutions of the Yang–Baxter equation through a differential approach. Two-state systems, J. High Energy Phys. 10 (2018) 110.

[29] F. Haake, *Quantum Signatures of Chaos* (Springer, Berlin, 2010).

[30] Note that the level-spacing distribution (LSD) should not be used as a definition: One can have chaotic LSD in integrable systems [33], or have integrable systems without Poisson statistics [34], or Poisson statistics in chaotic circuits with unresolved space-time symmetries [32].

[31] See Supplemental Material at http://link.aps.org/supplemental/10.1103/tqy8-ynpd for explicit construction of the antiunitary time-reversal symmetry in circuits with open boundary conditions, explicit expressions for the first two local conserved charges, and for additional discussion of the Ruelle-Pollicott spectrum, which includes Ref. [64].

[32] U. Duh and M. Žnidarič, Classification of same-gate quantum circuits and their space-time symmetries with application to the level-spacing distribution, Phys. Rev. Res. **6**, 023068 (2024).

[33] L. Benet, F. Leyvraz, and T. H. Seligman, Wigner-Dyson statistics for a class of integrable models, Phys. Rev. E **68**, 045201(R) (2003).

[34] M. V. Berry and M. Tabor, Level clustering in the regular spectrum, Proc. R. Soc. Lond. Ser. A **356**, 375 (1977).

[35] A. Hurwitz, Ueber die Erzeugung der Invarianten durch Integration, Nachr. Ges. Wiss. Goettingen, Math.-Phys. Kl. **1897**, 71 (1897).

[36] All matrices are written in a two-qubit basis ordered as $\{|0_1 0_2\rangle, |1_1 0_2\rangle, |0_1 1_2\rangle, |1_1 1_2\rangle\}$.

[37] T. Rakovszky, F. Pollmann, and C. W. von Keyserlingk, Diffusive hydrodynamics of out-of-time-ordered correlators with charge conservation, Phys. Rev. X **8**, 031058 (2018).

[38] V. Khemani, A. Vishwanath, and D. A. Huse, Operator spreading and the emergence of dissipative hydrodynamics under unitary evolution with conservation laws, Phys. Rev. X **8**, 031057 (2018).

[39] A. J. Friedman, A. Chan, A. De Luca, and J. T. Chalker, Spectral statistics and many-body quantum chaos with conserved charge, Phys. Rev. Lett. **123**, 210603 (2019).

[40] Let $h(\mathbf{b})$ span all U(1) invariant Hermitian operators acting on two qubits as parameters $\mathbf{b}$ are varied. Assuming it is integrable, we have, e.g., $h(\mathbf{b}) = \partial_u \check{R}(u, \mathbf{v_b})|_{u=0}$ for some unitary solution $\check{R}(u, \mathbf{v})$ of Eq. (3), depending on parameters u and $\mathbf{v}$. The challenge now lies in finding the functions $\tau_{u,\mathbf{v}}$ and $\mathbf{b}_{u,\mathbf{v}}$, such that $\check{R}(u, \mathbf{v}) = \exp[\mathrm{i}\tau_{u,\mathbf{v}} h(\mathbf{b}_{u,\mathbf{v}})]$, and this matrix spans *all* MC unitaries when u and $\mathbf{v}$ are varied. Put differently, one needs to find an integrable Trotterization [11] of the MC nearest-neighbor Hamiltonian, and then prove that such a Trotterization spans *all* homogeneous brickwork circuits.

[41] Note that in such Hamiltonians there are only three nontrivial parameters: The staggered field B cancels out due to invariance under one-site translations.

[42] E. Vernier, B. Bertini, G. Giudici, and L. Piroli, Integrable digital quantum simulation: Generalized Gibbs ensembles and Trotter transitions, Phys. Rev. Lett. **130**, 260401 (2023).

[43] P. Fendley, Strong zero modes and eigenstate phase transitions in the XYZ/interacting Majorana chain, J. Phys. A: Math. Theor. **49**, 30LT01 (2016).

[44] E. Vernier, H.-C. Yeh, L. Piroli, and A. Mitra, Strong zero modes in integrable quantum circuits, Phys. Rev. Lett. **133**, 050606 (2024).

[45] I. G. Gochev, Spin complexes in a bounded chain, JETP Lett. **26**, 127 (1977).

[46] D. Ruelle, Resonances in chaotic dynamical systems, Phys. Rev. Lett. **56**, 405 (1986).

[47] M. Pollicott, On the rate of mixing in axiom A flows, Invent. Math. **81**, 413 (1985).

[48] T. Prosen, Ruelle resonances in quantum many-body systems, J. Phys. A: Math. Gen. **35**, L737 (2002).

[49] M. Žnidarič, Momentum-dependent quantum Ruelle-Pollicott resonances in translationally invariant many-body systems, Phys. Rev. E **110**, 054204 (2024).

[50] T. Mori, Liouvillian-gap analysis of open quantum many-body systems in the weak dissipation limit, Phys. Rev. B **109**, 064311 (2024).

[51] J. A. Jacoby, D. A. Huse, and S. Gopalakrishnan, Spectral gaps of local quantum channels in the weak-dissipation limit, Phys. Rev. B **111**, 104303 (2025).

[52] C. Zhang, L. Nie, and C. von Keyserlingk, Thermalization rates and quantum Ruelle-Pollicott resonances: insights from operator hydrodynamics, arXiv:2409.17251.

[53] U. Duh and M. Žnidarič, Ruelle-Pollicott resonances of diffusive U(1)-invariant qubit circuits, arXiv:2506.24097.

[54] Y.-L. Zhang and V. Khemani, Asymmetric butterfly velocities in 2-local Hamiltonians, SciPost Phys. **9**, 024 (2020).

[55] P. Richelli, K. Schoutens, and A. Zorzato, Brick wall quantum circuits with global fermionic symmetry, SciPost Phys. **17**, 087 (2024).

[56] M. Kardar, G. Parisi, and Y.-C. Zhang, Dynamic scaling of growing interfaces, Phys. Rev. Lett. **56**, 889 (1986).

[57] M. Ljubotina, M. Žnidarič, and T. Prosen, Kardar-Parisi-Zhang physics in the quantum Heisenberg magnet, Phys. Rev. Lett. **122**, 210602 (2019).

[58] E. Ilievski, J. De Nardis, S. Gopalakrishnan, R. Vasseur, and B. Ware, Superuniversality of superdiffusion, Phys. Rev. X **11**, 031023 (2021).

[59] E. Sklyanin, Boundary conditions for integrable quantum systems, J. Phys. A: Math. Gen. **21**, 2375 (1988).

[60] N. Keenan, N. F. Robertson, T. Murphy, S. Zhuk, and J. Goold, Evidence of Kardar-Parisi-Zhang scaling on a digital quantum simulator, npj Quantum Inf. **9**, 72 (2023).

[61] K. Maruyoshi, T. Okuda, J. W. Pedersen, R. Suzuki, M. Yamazaki, and Y. Yoshida, Conserved charges in the quantum simulation of integrable spin chains, J. Phys. A: Math. Theor. **56**, 165301 (2023).

[62] E. Rosenberg *et al.*, Dynamics of magnetization at infinite temperature in a Heisenberg spin chain, Science **384**, 48 (2024).

[63] C. Jonay, J. F. Rodriguez-Nieva, and V. Khemani, Slow thermalization and subdiffusion in $U(1)$ conserving Floquet random circuits, Phys. Rev. B **109**, 024311 (2024).

[64] J. Bensa and M. Žnidarič, Fastest local entanglement scrambler, multistage thermalization, and a non-Hermitian phantom, Phys. Rev. X **11**, 031019 (2021).